

PACS numbers: 52.38.Kd; 52.50.Jm
DOI: 10.1070/QE2014v044n12ABEH015398

Effect of the laser spot shape on spatial distribution of the ion bunch accelerated in a superstrong field

V.M. Komarov, A.V. Charukhchev, A.A. Andreev, K.Yu. Platonov

Abstract. **We have investigated the effect of the laser spot shape on the spatial distribution of accelerated ions on the front and back sides of a thin target irradiated by a picosecond laser pulse having the intensity of (3–4) × 10^{18} W cm^{-2}. Experimental data are compared with numerical calculations. It is shown that the spatial structure of the ion bunch on the front side of the target resembles the laser spot structure rotated by 90°.**

Keywords: *acceleration of ions, superstrong field, spatial distribution of ions.*

1. Introduction

The studies on spatial scattering of ions accelerated in superstrong fields formed in the interaction of high-power (sub) picosecond pulses with thin targets is one of the most urgent tasks in the frame of designing laser-plasma accelerators of ions. One of the promising areas of practical use of such systems is associated with generation of ion bunches with the energies up to several tens or even hundreds of MeV [1–3]. Such bunches possess a relatively small (10°–15°) scattering angle and provide ionic currents that are several orders of magnitude higher compared to those implemented in the conventional accelerators [4]. These bunches are considered as a potentially effective tool for medical applications (radiation hadronic therapy of eye diseases and cancerous tumours of internals [5–7]), for radiography of objects with high spatial resolution [8], in ion lithography of complex objects [4] and for radioactive isotope production [9]. There are also projects of the use of laser accelerators as high-brightness injectors for conventional ion accelerators. Furthermore, such high-intensity bunches may also be used for implantation of the nanometre-width layers into the substance when producing composite materials and precision membranes [7].

The aim of this work was to determine the interrelation between the laser spot shape on the target and spatial distribution of accelerated ions on its front and back sides.

2. Experimental setup and measurement tools

The experiments were performed with the use of a picosecond PROGRESS-P laser [10] at a wavelength of 1.054 μm, energy of $\varepsilon_{las} \leqslant 18$ J and pulse duration of t_{las} =1.2–2 ps. The radiation focusing into a focal spot with the average diameter of $2r_{las} \leqslant 15–20$ μm was performed by means of an off-axis parabolic mirror with *f*/1.4. The laser radiation intensity on the target surface was (3–4) × 10^{18} W cm^{-2}. In these experiments, the contrast of power relative to the pulse of amplified luminescence did not exceed 10^{-8}, while the measurements of pre-pulse intensity in the range of 10–100 ps (before the fundamental one) by means of a single-pulse autocorrelator have shown its intensity to be below the detection threshold of that technique (less than 10^{-3}). It is worth noting that even in the case of upper estimates of the pre-pulse intensity (10^{-3}) and duration (100 ps), the expansion of a flat target under its impact does not exceed 5 μm, which is comparable with initial thickness of the target. In the case of the laser spot diameter of about 20 μm, the target remains flat and opaque to laser radiation after having been exposed to the action of a prepulse with maximal intensity.

The target representing a thin copper foil with the thickness of 3 to 30 μm was placed in two different positions – perpendicular and at an angle of about 45° to a p-polarised laser beam being focused. The measuring scheme is shown in Fig. 1.

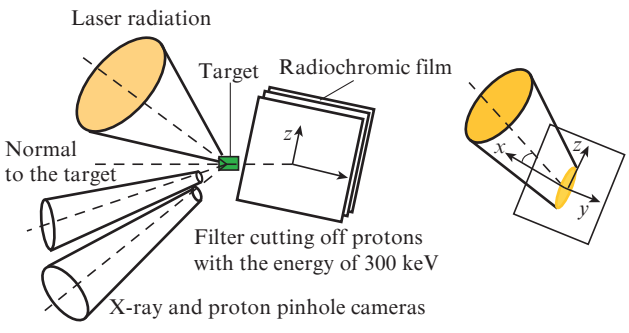

Figure 1. Experimental scheme of measurements; the target with coordinate system is on the right.

V.M. Komarov, A.V. Charukhchev Public Limited Company 'Scientific Research Institute for Optoelectronic Instrument Engineering', 188540 Sosnovyi Bor, Leningrad region, Russia;
A.A. Andreev Federal State Unitary Enterprise Scientific and Industrial Corporation 'Vavilov State Optical Institute', Birzhevaya liniya 12, 199034 St. Petersburg, Russia; ITMO University, Kronverskii prosp. 49, 197101 St. Petersburg, Russia; e-mail: alex2_andreev@yahoo.com;
K.Yu. Platonov Federal State Unitary Enterprise Scientific and Industrial Corporation 'Vavilov State Optical Institute', Birzhevaya liniya 12, 199034 St. Petersburg, Russia; St. Petersburg State Polytechnic University, Polytechnicheskaya ul 29, 195251 St. Petersburg, Russia

Received 31 January 2014; revision received 4 June 2014
Kvantovaya Elektronika **44** (12) 1104–1108 (2014)
Translated by M.A. Monastyrskiy

To evaluate the spatial distribution of the laser spot shape, a multichannel X-ray pinhole camera [11] with the apertures of 4–5 μm was used, enclosed by various filters in order to obtain the target image in the soft X-ray region of 1–1.5 keV. The measurements were performed with the use of a UV-4 photographic film.

Spatial scattering of ions accelerated in the front direction (along the normal to the target) was registered at the magnification of ~3.5 by a multichannel ionic pinhole camera with the apertures of 45 μm, enclosed by various lavsan and Al filters in order to allocate a certain interval of ion energies. The diameter of apertures was chosen to ensure the registration of a sufficient number of particles on the detector for obtaining the image estimates. Charged particles were detected in the pinholes by means of CR-39 track detectors calibrated by several types of ions (protons, C and Al) up to the energies of 5 MeV. The pinhole cameras were placed at a distance of 10–12 mm from the target, close to the normal to its surface.

Spatial distribution of the ion bunch behind the target was detected using the radiochromic HD-810 film, closed by a filter to cut off protons and heavier ions with the energies less than 300 keV. The radiochromic film changed its colour from clear to dark blue proportionally to the dose of the ionising radiation absorbed. The distance from the film to the target was about 15 mm.

The energy spectrum of accelerated ions was also measured with respect to the normal to the target by means of a spectrometer [11], which represented a cassette with a set of apertures closed by Al and CH_2 filters of various thicknesses (1.6–300 μm). This made it possible to cut off the proton energy range of 0.3–35 MeV. It should be noted that, as shown by numerous experiments including ours [11], protons are the most represented fraction in the flow regardless of the target used. Their source is various hydrocarbon impurities and vapours of water deposited on the target surface. Spectral measurements were performed to calibrate the model used in the calculations to describe the main experimental results.

3. Experimental results and analysis

During the action of an intense (more than 10^{18} W cm^{-2}) (sub) picosecond laser pulse, the main fraction of the laser energy absorbed in the skin-layer is transformed into the energy of hot electrons propagating inside the target or located in vacuum over its front side. The electrons moving into the depth ionise the target material, thus producing plasma with secondary, colder electrons. As shown in [12], the temperature of cold electrons in plasma, which determines the degree of ionisation of the target atoms, may amount to a few keV at the intensity under discussion. The mean free path of the fast electrons is significantly greater than the target thickness, so that the flux of hot electrons comes out on the back side of the target. During the output of electrons in vacuum from the front and back sides of the target, its surfaces become positively charged, thereby giving rise to strong electric fields that hold hot electrons near surfaces at a distance of Debye radius r_D [13]. The estimates of the temperature and concentration of hot electrons give $r_D \approx 2$ μm. The electric field that is incident on the target surface causes the breakaway and acceleration of protons located on the surface of the copper target in the form of water vapours adsorbed from air up to the energies greater than 1 MeV. During the laser pulse action, hot electrons propagate along the surface of the target area beyond the laser spot, so that the size of the spot of hot electrons and hence of the proton emission region exceeds the laser spot size. In our case (with the target thickness of 3 μm) the transverse diffusion of the electron spot is weaker than in thin (of the order of wavelength) and ultrathin targets. Accordingly, the spot size of hot electrons is several times greater than that of the laser spot. The spot shape of hot electrons thus resembles the shape of the laser spot. Obviously, the shapes of the clouds of cold and hot electrons are similar since the cold electrons are secondary to the hot ones and appear during their propagation beyond the laser spot. Thus, the geometric spot shape of the X-ray emission of thermal (cold) electrons of the laser target through the laser radiation – hot electrons – cold electrons – X-ray emission chain should resemble the laser spot shape. The spot shape of proton emission from the target surface also resembles the laser spot shape, but the final shape of the proton bunch is formed at the times that significantly exceed the laser pulse duration. During the laser pulse (1–2 ps) action, a proton with the energy of 1 MeV travels a distance of ~10 μm. Its angle of departure from the target is small (~10°), and the projection of this distance onto the target plane is also small, i.e., several micrometres. The period of time of tens of picoseconds, which significantly exceeds the laser pulse duration, is needed to significantly change the cloud of protons with the transverse size larger than 20 μm. Thus, the formation time of the transverse spot shape of the X-ray emission is comparable with the laser pulse duration, while the formation of the transverse distribution of the proton bunch requires significantly (dozens of times) more time.

Figure 2 shows the X-ray image of the laser spot and the spatial image of the distribution of proton scattering towards the front side at the normal and oblique incidence of laser radiation onto the target. It is seen that, at normal incidence onto the target, the shape of the ion generation region is close

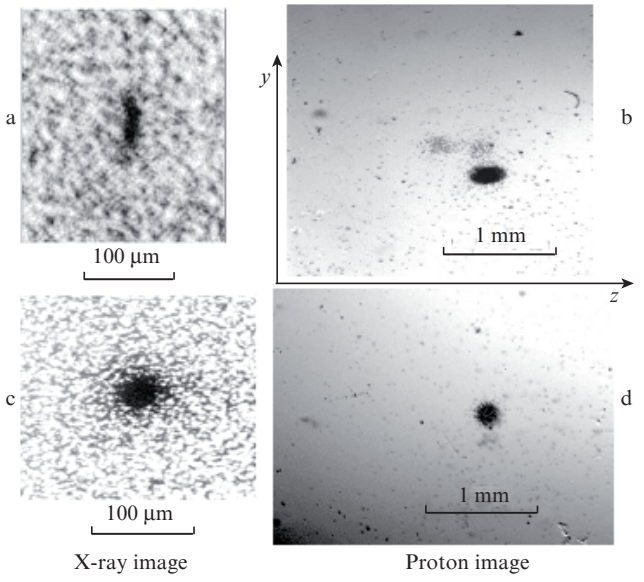

Figure 2. (a, c) Results of measuring the shape and size of the laser spot and (b, d) the shape and size of the ion generation region (the energy range 300 keV–1.9 MeV) on the front surface of the target at (a, b) oblique, 45°, and (c, d) normal incidence of laser radiation onto the 15-μm-thick target. The coordinate system is similar to that shown in Fig. 1.

to the laser spot shape, whilst the size of the ion generation region is much larger than the average diameter of the laser spot. At the same time, at oblique incidence, the ion generation region is elliptical similarly to the X-ray image of the laser spot, but rotated by about 90° relative to the laser spot.

A completely different situation arises in the case of scattering of the ions accelerated in the direction behind the target [7]. Figure 3 shows the projection images [8] of ion scattering behind the targets for various target thicknesses and laser spot shapes, similar to those represented in Fig. 2, in the case of oblique incidence of laser radiation. The distance from the target to the detector is 15 mm. It can be seen that, regardless of the target thickness, the shape of the ion generation region is close to a circle and virtually independent of the laser spot shape.

To explain the experimentally obtained transverse spatial distributions of the ion bunch, the decisive role belongs to the space charge distribution of electrons emitted into vacuum from the front side of the foil. According to the measurements of the distribution of thermal X-ray radiation (see Fig. 2, oblique incidence), the shape of the cloud of hot electrons repeats the laser spot shape. Accordingly, at the start of the acceleration process the transverse distribution of the ion bunch acquires the same profile. After the ion front moves away from the surface to a distance of several Debye radii, charges relax, an ambipolar field decreases, electrons cool down and an extended quasi-neutral plasma bunch is formed. As was shown above, the time of change in the transverse shape of the proton bunch substantially exceeds the laser pulse duration. The ion bunch evolution on this time scale is described by the equations of hydrodynamics for adiabatic expansion of plasma. Using the hydrodynamic description of the plasma motion instead of the kinetic one (ignoring the distribution of protons in energies) leads to the determination of average characteristics of proton motion and therefore has a qualitative nature. However, the hydrodynamic approach is valid for description of the geometric shape of a hot plasma cloud, and is used, for example, in [14].

Anisimov and Lysikov [14] present the solution of the hydrodynamic equations for the plasma bunch having the initial form of an elongated triaxial ellipsoid with an arbitrary ratio of the lengths of semi-axes:

$$\rho(\boldsymbol{r},t) = \frac{M}{I_1(\gamma)XYZ}[\psi(x,y,z,t)]^{1/(\gamma-1)},$$

$$\psi(x,y,z,t) = 1 - \frac{x^2}{X^2(t)} - \frac{y^2}{Y^2(t)} - \frac{z^2}{Z^2(t)}, \qquad (1)$$

$$P(\boldsymbol{r},t) = \frac{E}{I_2(\gamma)XYZ}\left[\frac{X_0Y_0Z_0}{XYZ}\right]^{\gamma-1}[\psi(x,y,z,t)]^{\gamma/(\gamma-1)},$$

$$v_x(\boldsymbol{r},t) = \frac{\dot{X}(t)x}{X(t)},\ v_y(\boldsymbol{r},t) = \frac{\dot{Y}(t)y}{Y(t)},\ v_z(\boldsymbol{r},t) = \frac{\dot{Z}(t)z}{Z(t)},$$

where ρ, P and v are the density, pressure and hydrodynamic velocity of plasma; $I_{1,2}(\gamma)$ are the normalisation factors; and X, Y, Z and X_0, Y_0, Z_0 are the lengths of semi-axes of the ellipsoid at the arbitrary and initial time moments, respectively.

The Cartesian coordinate system (x,y,z) used in (1) is shown on the right in Fig. 1.

According to [14], the evolution of the lengths of semi-axes of the ellipsoid is described by the Newtonian equations of motion

$$\ddot{X} = \frac{\partial U}{\partial X},\ \ddot{Y} = \frac{\partial U}{\partial Y},\ \ddot{Z} = \frac{\partial U}{\partial Z} \qquad (2)$$

with the effective potential energy

$$U = \frac{5\gamma-3}{\gamma-1}\frac{E}{M}\left[\frac{X_0Y_0Z_0}{XYZ}\right]^{\gamma-1}. \qquad (3)$$

Here $E = N_i\varepsilon_{eh}$ is the total thermal energy of the plasma cloud; $M = N_i m_p$ is its mass; and $\gamma = 5/3$ is the adiabatic index. Hereinafter, the evolution of semi-axes depends on the ratio E/M, and so the total amount of ions N_i in the bunch does not require additional definition.

Let us choose the values visible in the X-ray image of the emission spot (Fig. 2a) as the initial sizes for the ellipse semi-axes. These are the initial length of the semi-axis Y (big semi-axis of the profile), $Y_0 = 40$ μm; initial length of the semi-axis Z (minor semi- axis of the distribution), $Z_0 = 10$ μm; and initial length of the semi-axis X (ellipsoid height, invisible in Fig. 2a), $X_0 \approx 5r_D = 10$ μm. Herewith, the characteristic ratio of the transverse dimensions $Y_0:Z_0$ amounts to 4:1, which corresponds to the emission spot profile in Fig. 2.

Obviously, the initial velocities of the ellipsoid semi-axes are as follows:

$$\dot{X}(0) = \sqrt{2\varepsilon_i/m_i},\ \dot{Y}(0) = \dot{Z}(0) = 0. \qquad (4)$$

Here $\varepsilon_i = 0.8$ MeV is the average energy of ion (proton) spectra measured on the front side of the target (Fig. 4). It should be noted that, as shown in [7, 11], the spectrum of accelerated

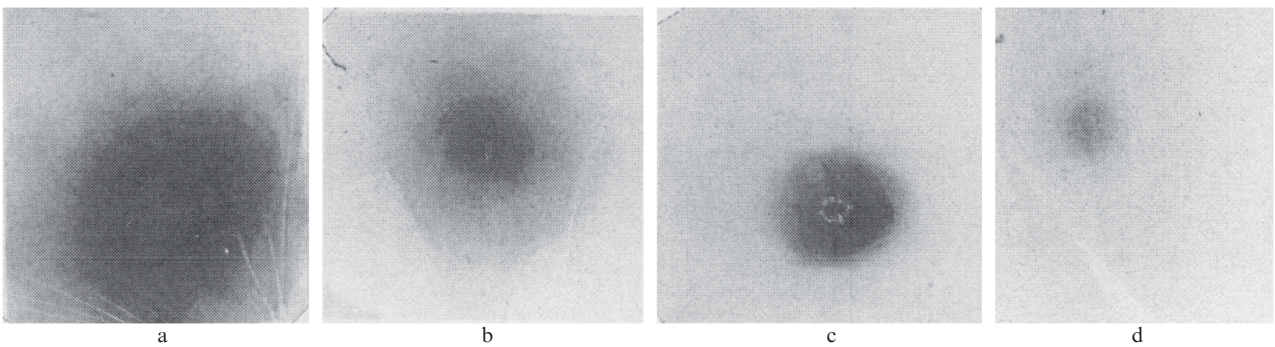

Figure 3. Spatial distribution of ion scattering on the back side of a Cu target with the thickness of (a) 3, (b) 7, (c) 15 and (d) 30 μm. The frame size is 25 × 25 mm, the distance from the target to the detector is 15 mm.

ions on the back side of the target is insignificantly different from the spectrum of ions on its front side. Numerical solution of equations (2) with the initial conditions given above is presented in Fig. 5. The dimensionless time on the x axis is normalised to the characteristic time $Z_0\sqrt{M/E}$, i.e. $\tau = t\sqrt{E/M}/Z_0$. The lengths of the ellipsoid semi-axes X, Y, Z on the ordinate axis are normalised to the value of Z_0. As is seen from Fig. 5, the minor semi-axis X having the larger initial velocity possesses a higher rate of expansion. In the transverse plane yz, the minor axis Z also increases most rapidly, which results in the rotation by 90° of the initial transverse distribution of ions, and at large times the ellipsoid in transverse direction turns out extended along the z axis instead of the y axis. At large times, the ellipsoid semi-axes grow linearly in time, with the length of the semi-axis X, which corresponds to the maximum initial density gradient, increasing most rapidly. The ratio of the lengths of the semi-axes Y and Z in the transverse direction at large times tends to a constant limit, which in our case is

$$Y(\infty)/Z(\infty) = 0.45. \tag{5}$$

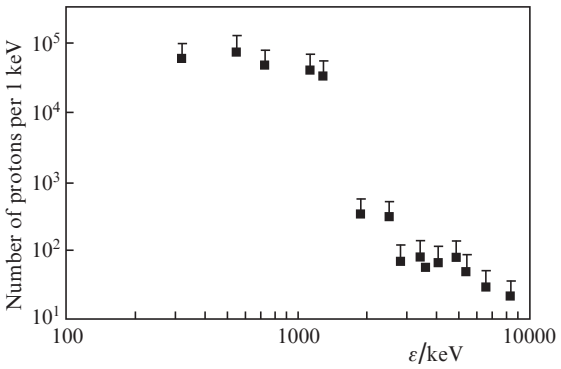

Figure 4. Spectrum of protons on the front side of the target.

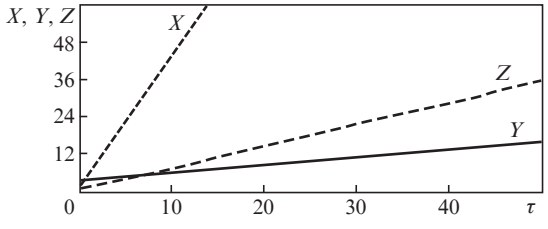

Figure 5. Temporal evolution of the ellipsoid semi-axes. Dimensionless time on the abscissa axis is $\tau = t\sqrt{E/M}/Z_0$; the lengths of the ellipsoid semi-axes X, Y, Z on the ordinate axis are normalised to $Z_0 = 10$ μm.

Ratio (5) is close to the experimental value of 0.6 calculated in accordance with the ion spot shape on the detector (see Fig. 2a). Figure 5 also allows one to estimate two characteristic emission angles of protons in the zx and yx planes, constituting 0.2 and 0.1 rad, respectively.

In our experiment, the proton pinhole camera (see Fig. 1) intercepted only a fraction of the entire ion flux coming from the front side of the target. Because the pinhole aperture had the diameter $d_{ob} = 45$ μm, and the camera itself was removed to the distance of $x_{ob} = 10^4$ μm, only protons emitted at small angles to the target normal (the pinhole camera was oriented along the normal) fell into the camera. Therefore, we define the transverse profile of the proton bunch directly at the pinhole aperture. The proton flux density $j_x(x,y,z,t)$ in the lens aperture ($x = x_{ob}$) is determined by the obvious formula:

$$j_x(x_{ob},y,z,t) = \begin{cases} \rho(x_{ob},y,z,t)v_x(x_{ob},y,z,t), & t \geqslant t_{ob}(z,y) \\ 0, & t < t_{ob}(z,y). \end{cases} \tag{6}$$

Here $t_{ob}(z,y)$ is the time moment, at which the outer boundary of the expanding plasma cloud reaches the surface $x = x_{ob}$ of the pinhole lens at the point with coordinates (z,y). Obviously, this time moment satisfies the equation $\psi(x_{ob},y,z,t_{ob}) = 0$. By integrating (6) from the time moment $t_{ob}(z,y)$ to infinity, it is possible to obtain the transverse distribution of the surface density (g cm^{-2}) of protons in the pinhole lens

$$\sigma(y,z) = \int_{t_{ob}(y,z)}^{\infty} \rho(x_{ob},y,z,t)v_x(x_{ob},y,z,t)\,dt, \qquad y^2 + z^2 \leqslant \left(\frac{d_{ob}}{2}\right)^2. \tag{7}$$

The level lines $\sigma(y,z) = \text{const}$ determine the proton bunch shape visible by the pinhole. Because $x_{ob} \gg d_{ob}$, the time $t_{ob}(y,z)$ is almost independent of (y,z) and can be estimated as $t_{ob} \approx x_{ob}\sqrt{M/E}$. This time is much greater than the characteristic times $Y_0\sqrt{M/E}$, $Z_0\sqrt{M/E}$ of the ellipsoid expansion and by the time t_{ob}, ratio (5) between the ellipsoid axes turns out already established. It is easy to see that the dependence on (z,y) in integral (7) is only contained in the form of the argument $y^2/Y^2(t) + z^2/Z^2(t)$ of the function ρ. Throughout the range of integration over time, we have in (7) $Y(t)/Z(t) \approx U(\infty)/Z(\infty)$. Consequently, the level lines of the function $\sigma(y,z)$ resemble the shape of the plasma ellipse, with the ratio of semi-axes defined by (5). Thus, the proton pinhole allows one to determine the shape of the transverse cross section of the proton bunch, despite the fact that not all protons of the plasma cloud fall into the pinhole aperture.

With regard to the acceleration of ions on the back surface of the target, the use of the approach described above leads to the fact that, due to the scattering of the flow of electrons that cause ion acceleration, spatial distribution of the ion flux becomes rotationally symmetric, so that $Y = Z$, and the anisotropy of ion scattering decreases sharply with increasing target thickness.

Thus, the presence of the elongated laser spot on the front side of the target leads to the fact that the transverse distribution of accelerated ions becomes also elongated and, in addition, rotated by 90°. The scattering of the electron flow inside the target gives rise to the axial symmetry of the accelerating field and symmetrisation of the scattering of accelerated ions [7].

References

1. Norreys P.A. et al. *Plasma Phys. Control. Fusion*, **40**, 1237 (1998).
2. Maksimchuk A. et al. *Phys. Rev. Lett.*, **84**, 4108 (2000).
3. Beg F.N., Bell A.R., Dangor A.E., et al. *Phys. Plasmas*, **4** (2), 447 (1997).
4. Cowan T.E. et al. *Phys. Rev. Lett.*, **92**, 204801 (2004).
5. Bulanov S.V. et al. *Plasma Phys. Rep.*, **28**, 453 (2002).
6. Esirkepov T. et al. *Phys. Rev. Lett.*, **89**, 175003 (2002).
7. Daido H., Nishiuchi M., Pirozhkov A. *Rep. Progr. Phys.*, **75**, 056401 (2012).

8. Andreev A.A., Komarov V.M., Charukhchev A.V., Platonov K. Yu. *Pis'ma Zh. Tekh. Fiz*., **33**, 23 (2007).
9. Ledingham K., McKenna P., Singhal R. *Science*, **300**, 1107 (2003).
10. Borodin V.G., Komarov V.M., Malinov V.A., et al. *Kvantovaya Elektron*., **29**, 101 (1999) [*Quantum Electron*., **29**, 939 (1999)].
11. Andreev A.A., Komarov V.M., Charukhchev A.V., et al. *Pis'ma Zh. Eksp. Teor. Fiz*., **79**, 400 (2004).
12. Andreev A.A., Zapysov A.I., Charukhchev A.V., Yashin V.E. *Izv. Ross. Akad. Nauk, Ser. Fiz*., **63**, 1237 (1999).
13. Bychenkov V.U., Kovalev V.F. *Kvantovaya Elektron*., **35**, 1143 (2005) [*Quantum Electron*., **35**, 1143 (2005)].
14. Anisimov S.I., Lysikov Yu.V. *J. Appl. Math. Mech*., **34**, 882 (1970).